Low-complexity Rotated QAM Demapper for the Iterative Receiver Targeting DVB-T2 Standard

YouZhe Fan and Chi-ying Tsui
Department of Electronic and Computer Engineering
The Hong Kong University of Science and Technology, Clear Water Bay, Hong Kong
Email: {jasonfan, eetsui}@ust.hk

***Abstract*—Gray mapping and signal space diversity (SSD) are adopted in DVB-T2 to achieve better performance and system robustness. However, the traditional maximum a posteriori demapping for Gray mapped SSD signal is complicated for higher order modulation and it is not practical to be used in the iterative receiver structure. In this work, simplified demappers are proposed by approximating the 2-dimensional detection with 1-dimensional detection and compensating the loss due to the correlation between the I and Q components. Simulation results show that the proposed simplified demappers can approach the optimal demapper performance with a much lower complexity.**

I. Introduction

Bit-interleaved coded modulation (BICM) [1] has become the most popular coded modulation scheme for its superior performance. With coordinate interleaving and rotation of the constellation, also known as the signal space diversity (SSD) [2], the diversity order and hence the performance of the BICM scheme can be greatly improved in the multipath fading channel [3]. Therefore, BICM-SSD has been adopted in the second generation terrestrial digital video broadcasting (DVB-T2) [4] standard as an efficient method to improve the system robustness against terrestrial channels. At the same time, DVB-T2 standard adopts low-density parity-check (LDPC) code [5] as the forward error correction code, due to its strong error correcting capability and low decoding complexity [6].

Generally, there are two types of receiver for BICM system: non-iterative [1] and iterative [7]. The non-iterative receiver serially concatenates a maximum likelihood (ML) demapper with a channel decoder. Iterative receivers are proposed in [8] and [9] based on iterative feedback between the demapper and the channel decoder. Compared with the non-iterative structure, the iterative structure achieves a better performance at the cost of a higher complexity [10]. Due to the better performance under both the iterative and non-iterative receivers for BICM-LDPC system [4], [10], Gray mapping is adopted in the DVB-T2 standard [11] and iterative receiver is also recommended for its superior performance.

To reduce the complexity of the iterative receiver in BICM-LDPC system, [12] and [13] proposed to unroll the LDPC decoding and merge the maximum a posteriori (MAP) demapper into each LDPC decoding iteration. This minimizes the overall decoding iterations at the expense of increasing the number of MAP demappings. The overall complexity is reduced when the MAP demapping complexity is much less than that of LDPC decoding. This is true for the traditional Gray mapped signal, since its detection is reduced to one dimension. However, with SSD technique, the independence between the signal's in-phase (I) and quadrature (Q) components is broken [4] and the MAP demapper has to execute a two-dimensional detection of which the complexity is exponential to the modulation order. For higher order modulation, such as 256QAM that supported in DVB-T2 [11], its complexity is comparable to that of the corresponding LDPC decoder [13]. Therefore, to realize a low power and area efficient implementation of the iterative receiver, it is highly desirable to simplify the MAP demapper for the DVB-T2 system.

Two methods were proposed for the demapper simplification recently. The first is reducing the constellation space by only considering the candidates inside a sub-region determined by the constellation quadrant that the receiving signal falls in [14], [15]. However this method is not directly applicable for the iterative receiver [16] where the apriori information from the channel decoder has to be considered. At the same time, the complexity is still too high as the complexity reduction is only linear. The second one operates as a multi-user detector [17], [18], which regards the constellation point as the superposition of BPSK signals mapped by different bits. However, this method is only applicable for certain mapping strategies and Gray mapping is not one of them. Since the existing methods can not well simplify the MAP demapper for the DVB-T2 receiver, a novel method is proposed in this paper. Regarding that the Gray mapped signal without SSD can be separately demapped as two pulse-amplitude modulation (PAM) signals with much lower complexity, in the proposed receiver, a series of post processing operations are executed such that the I and Q components of the received SSD signals can also be separately demapped. However this separate demapper (SD) does not exploit the joint information existing in the I and Q correlation due to SSD. To maintain a good performance when I and Q are strongly correlated, coupling detector (CD) and iterative CD based on the post processed signal are proposed to estimate and compensate this correlation information Simulation results show that the simplified demappers proposed in this work facilitate the implementation of DVB-T2 iterative receiver with good complexity and performance trade-off.

II. System Model

The BICM-LDPC transmitter with SSD consists of a concatenation of a binary (N, K) LDPC code encoder, a bit

978-1-4673-1881-5/12/$31.00 ©2012 IEEE

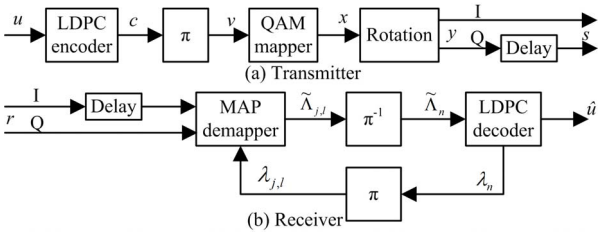

Fig. 1. The BICM-LDPC with SSD

interleaver (π), and a SSD mapper. As depicted in Fig. 1(a), the information bits $u_k\,(k = 1, 2, \ldots, K)$ are encoded by a LDPC encoder. After that, the coded bits $c_i\,(i = 1, 2, \ldots, N)$ from the same codeword are interleaved and then passed to a SSD mapper. In the SSD mapper, the coded bits from each of the $J = N/\log_2 M$ group are firstly mapped to M-QAM constellation χ under Gray mapping, where $j = 1, 2, \ldots, J$ is the time index. The QAM symbol x_j is then rotated by an angle α to form the rotated symbol y_j in constellation Ω and its I and Q components are interleaved by a delay of one component with respect to the other [13]. Therefore, the transmitted symbol is given by

$$\begin{bmatrix} \mathfrak{Re}\,(s_j) \\ \mathfrak{Im}\,(s_{j+d}) \end{bmatrix} = \mathbf{R} \begin{bmatrix} \mathfrak{Re}\,(x_j) \\ \mathfrak{Im}\,(x_j) \end{bmatrix} \tag{1}$$

where d is the delay time for the Q component, and $\mathfrak{Re}$ and $\mathfrak{Im}$ are the real and imaginary parts of a complex number, respectively. $\mathbf{R}$ is the rotation matrix defined as

$$\mathbf{R} = \begin{bmatrix} \cos\alpha & -\sin\alpha \\ \sin\alpha & \cos\alpha \end{bmatrix}. \tag{2}$$

Assume the signal s_j is transmitted through a fast flat fading channel. With coherent detection, the channel phase distortion is compensated and the received signal r_j has the form

$$r_j = \rho_j s_j + n_j \tag{3}$$

where ρ_j is the Rayleigh distributed fading coefficient with $E\left(\rho_j^2\right) = 1$ and n_j is an additive white Gaussian noise (AWGN) with zero mean and variance $N_0/2$ in each component. It is assumed in this work that perfect channel state information, i.e. ρ_j, is available at the receiver.

The iterative receiver shown in Fig. 1(b) is based on the turbo principle. At the beginning, the I component of the received signal r_j is firstly delayed by d such that the I and Q input to the MAP demapper both store the information of x_j. After that, extrinsic information λ_n / $\tilde{\Lambda}_n$ is iteratively exchanged between the MAP demapper and the LDPC decoder.

Based on the channel output and the apriori log-likelihood ratio (LLR)

$$\lambda_{j,l} = \log \frac{\Pr\left(c_{j,l} = 1\right)}{\Pr\left(c_{j,l} = 0\right)} \quad l = 1, 2, \ldots, \log_2 M \tag{4}$$

from the channel decoder, the MAP demapper outputs the extrinsic information $\Lambda_{j,l}$. It is used as the apriori information

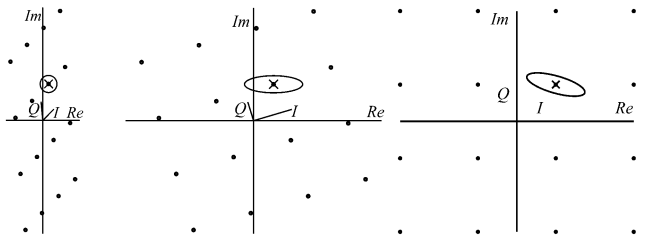

(a) Signal r (b) Normalized signal (c) Rotated signal

Fig. 2. Signal model of 16QAM

in the LDPC decoder after de-interleaving and given by [4]

$$\begin{aligned} \Lambda_{j,l} &= \log\left(\sum_{y_j\in\Omega_{j,l}^1} \exp\left[\mathrm{LLh}\,(y_j) + \sum_{q\neq l \text{ and } c_{j,q}=1} \lambda_{j,q}\right]\right) \\ &\quad - \log\left(\sum_{y_j\in\Omega_{j,l}^0} \exp\left[\mathrm{LLh}\,(y_j) + \sum_{q\neq l \text{ and } c_{j,q}=1} \lambda_{j,q}\right]\right) \end{aligned} \tag{5}$$

where $\Omega_{j,l}^1$ and $\Omega_{j,l}^0$ are the subsets of Ω such that $\Omega_{j,l}^b = \{y \in \Omega \mid c_{j,l} = b\}$, and $c_{j,q}\,(q = 1, 2, \ldots, \log_2 M)$ are the bits mapping to y_j. $\mathrm{LLh}\,(y_j)$ is the log-likelihood value of the hypothesis y_j given the real part of r_j and the imaginary part of r_{j+d}, and is given as

$$\mathrm{LLh}\,(y_j) = -N_0^{-1}\left[\mathfrak{Re}\,(r_j - \rho_j y_j)^2 + \mathfrak{Im}\,(r_{j+d} - \rho_{j+d} y_j)^2\right] \tag{6}$$

Using the max-log approximation [6], (6) is approximated as

$$\begin{aligned} \tilde{\Lambda}_{j,l} &= \min_{y_j\in\Omega_{j,l}^0}\left\{-\mathrm{LLh}\,(y_j) - \sum_{q\neq l \text{ and } c_{j,q}=1} \lambda_{j,q}\right\} \\ &\quad - \min_{y_j\in\Omega_{j,l}^1}\left\{-\mathrm{LLh}\,(y_j) - \sum_{q\neq l \text{ and } c_{j,q}=1} \lambda_{j,q}\right\}. \end{aligned} \tag{7}$$

Compared with (5), (7) simplifies the non-linear function in (5) and the summation over $\Omega_{j,l}^b$. However, evaluating M candidates for each bit demapping is still expensive. With the following transformation

$$\begin{aligned} \tilde{\Lambda}_{j,l} &= \min_{y_j\in\Omega_{j,l}^0}\left\{-\mathrm{LLh}\,(y_j) - \sum_{c_{j,q}=1} \lambda_{j,q}\right\} \\ &\quad - \min_{y_j\in\Omega_{j,l}^1}\left\{-\mathrm{LLh}\,(y_j) - \sum_{c_{j,q}=1} \lambda_{j,q}\right\} - \lambda_{j,l}, \end{aligned} \tag{8}$$

the candidate evaluation $-\mathrm{LLh}\,(y_j) - \sum_{c_{j,q}=1} \lambda_{j,q}$ is shared over all the bits from one symbol, and the evaluation complexity decreases by $\log_2 M$. However, the cardinality of the searching space $|\Omega| = M$ is still too large for higher order modulation for a reasonable complexity. Thus, two simplified detectors are introduced in the next section to reduce this cardinality and the overall complexity.

III. Simplified Demappers

A. Post Processing Operations

Fig. 2(a) shows an example constellation of the received signal r in (3) when χ is 16QAM. The circle denotes the contour of r's probability density, assuming that the marked symbol is transmitted. From this example, it can be observed that the I and Q components of the received symbol is no

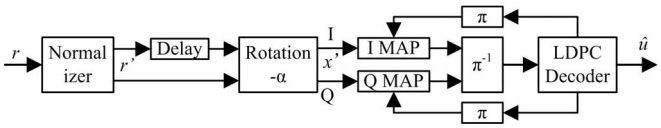

Fig. 3. Post processing and separate demapper

longer orthogonal to each other due to the unequal fading in the real and imaginary components. As a result, r is in an orthogonal coordinate constructed by $\mathfrak{Re}$ and $\mathfrak{Im}$ while the symbol constellation points lie in a non-orthogonal coordinate constructed by I and Q. This makes the signal detection difficult. Therefore, the real and the imaginary parts of the received signal are firstly normalized with its own fading coefficients as shown in Fig. 2(b)

$$r'_j = \frac{r_j}{\rho_j} = s_j + \frac{1}{\rho_j} n_j,\ j = 1, 2, \ldots J. \tag{9}$$

Afterward, r' is rotated back by an angle $-\alpha$ as

$$\begin{bmatrix} \mathfrak{Re}\left(x'_j\right) \\ \mathfrak{Im}\left(x'_j\right) \end{bmatrix} = \mathbf{R}^{-1} \begin{bmatrix} \mathfrak{Re}\left(r'_j\right) \\ \mathfrak{Im}\left(r'_{j+d}\right) \end{bmatrix}, \tag{10}$$

to unify the two coordinate systems as shown in Fig. 2(c).

After the coordinate transformation, each component of x' can be viewed as a PAM signal under Gray mapping and separately demapped by using (8) in the PAM constellation, if only the marginal distribution is considered. The block diagram of concatenating the post processing structure with the two PAM demappers is shown in Fig. 3. As the two-dimensional QAM constellation reduces to two one-dimensional PAMs, the corresponding log-likelihood calculation in (6) is realized as

$$\mathrm{LLh}\left(x_j^{br}\right) = -0.5\sigma'^{-2}_{br}\left(x'^{br}_j - x_j^{br}\right)^2 \tag{11}$$

where $br \in \{\mathrm{I}, \mathrm{Q}\}$ depends on the PAM signal under detection and σ'^2_{br} is the noise variance of the corresponding component whose computation will be given in the following sub-section. Meanwhile, the cardinality of the sets $\Omega^0_{j,l}$ and $\Omega^1_{j,l}$ in (8) reduces from $M/2$ to $\sqrt{M}/2$ for the PAM MAP demapper.

However, it can be noticed that the circular contour in Fig. 2(a) becomes an ellipsoid in Fig. 2(c) after the post processing. It indicates a correlation between the noises in the I and Q components of the post processed signal. This correlation makes the detections of the I and Q components depend on each other. If the separate demapper (SD) in Fig. 3 is directly used for the SSD signal, this correlation information is not taken into consideration and the performance will be degraded. Therefore, CD and iterative CD are proposed in the next two sub-sections to exploit this correlation information.

B. Coupling Detector

Under Gray mapping, the I and Q components of the signal x' in Fig. 3 are correlated through the noises. Thus, to exploit this correlation information, the noise property is firstly analyzed. Based on (9) and (10), the complex noise $n'^I_j + jn'^Q_j$ at the rotation module output in Fig. 3 is given by

$$\begin{bmatrix} n'^I_j \\ n'^Q_j \end{bmatrix} = \mathbf{R}^{-1} \begin{bmatrix} \frac{1}{\rho_j} & 0 \\ 0 & \frac{1}{\rho_{j+d}} \end{bmatrix} \begin{bmatrix} n^I_j \\ n^Q_{j+d} \end{bmatrix} = \mathbf{R}^{-1}\mathbf{\Phi} \begin{bmatrix} n^I_j \\ n^Q_{j+d} \end{bmatrix} \tag{12}$$

where $n_j = n^I_j + jn^Q_j$ is the channel noise in (3) and $\mathbf{\Phi}$ is the fading normalization matrix. Therefore, $\left[n'^I_j\ n'^Q_j\right]^T$ is jointly zero-mean Gaussian and its covariance matrix $\mathbf{C}_j$ is given by

$$\mathbf{C}_j = \frac{1}{2}\mathbf{N_0}\mathbf{R}^{-1}\mathbf{\Phi}^2\mathbf{R}. \tag{13}$$

From $\mathbf{C}_j$, the marginal variance,σ'^2_{br}, used in (11) and the correlation coefficient γ_j between n'^I_j and n'^Q_j can be found.

Since x' in Fig. 3 is a sufficient statistics for signal detection, $\mathrm{LLh}\left(y_j\right)$ in (8) is equivalent to $\mathrm{LLh}\left(x_j\right)$ based on x', where y_j is the rotated signal of x_j in Fig. 1(a). Based on Bayes' rule,

$$\mathrm{LLh}\left(x_j^I + jx_j^Q\right) = \mathrm{LLh}\left(x_j^{br}\right) + \mathrm{LLh}\left(x_j^{\bar{br}} \mid x_j^{br}\right) \tag{14}$$

and

$$\mathrm{LLh}\left(x_j^{br}\right) = -0.5\sigma'^{-2}_{br}\left(x'^{br}_j - x_j^{br}\right)^2 \tag{15}$$

$$\mathrm{LLh}\left(x_j^{\bar{br}} \mid x_j^{br}\right) = -\frac{\left[x'^{\bar{br}}_j - x_j^{\bar{br}} - \gamma_j \frac{\sigma'_{\bar{br}}}{\sigma'_{br}}\left(x'^{br}_j - x_j^{br}\right)\right]^2}{2\left(1-\gamma_j^2\right)\sigma'^2_{\bar{br}}} \tag{16}$$

where $br \in \{\mathrm{I},\mathrm{Q}\}$, and $\bar{br}$ denotes the complement of br. $\mathrm{LLh}\left(x_j^{\bar{br}} \mid x_j^{br}\right)$ is the log-likelihood of $x_j^{\bar{br}}$ conditioned on that x_j^{br} is transmitted over component br. Under Gaussian distribution, it is easy to observe from (16) that $\gamma_j \frac{\sigma'_{\bar{br}}}{\sigma'_{br}}\left(x'^{br}_j - x_j^{br}\right)$ is the mean offset estimation of $n'^{\bar{br}}_j$ based on the noise knowledge of the alternative component $\left(x'^{br}_j - x_j^{br}\right)$.

If x_j^{br} is perfectly known, a perfect knowledge of the noise in br will generate an accurate mean offset estimation for the $\bar{br}$ component. It indicates that some information in br is used to assist the $\bar{br}$ detection. Therefore, we denote $\gamma_j \frac{\sigma'_{\bar{br}}}{\sigma'_{br}}\left(x'^{br}_j - x_j^{br}\right)$ as the coupling term (CT). It is the CT that makes the SD of the SSD signal inaccurate. The CT is scaled by the correlation coefficient. When there is no correlation between I and Q, $\gamma_j = 0$, $\mathrm{LLh}\left(x_j^{\bar{br}} \mid x_j^{br}\right) = \mathrm{LLh}\left(x_j^{\bar{br}}\right)$ and (14) becomes

$$\mathrm{LLh}\left(x_j^I + jx_j^Q\right) = \mathrm{LLh}\left(x_j^I\right) + \mathrm{LLh}\left(x_j^Q\right). \tag{17}$$

By substituting (17) into (8), the MAP demapper is ready to be realized by the SD. Under weak correlation, the difference between (14) and (17) is small, hence the SD still works well. However, this difference gets larger when the correlation becomes stronger. In the higher correlation, the SD is no longer applicable and the CD is proposed.

To demap a certain bit in the br component from x'_j, $\mathrm{LLh}\left(x_j^{br} \mid x_j^{\bar{br}}\right)$ for the PAM constellation instead of $\mathrm{LLh}\left(x_j\right)$ for the QAM constellation in (8) can be used if $x_j^{\bar{br}}$ is perfectly known, because all the information of this bit contained in $\bar{br}$ has been passed to br through the CT in $\mathrm{LLh}\left(x_j^{br} \mid x_j^{\bar{br}}\right)$. In this case, a one-dimensional PAM demapper is sufficient to demap this bit. Thus, in the CD structure, the transmitted $x_j^{\bar{br}}$ is estimated first, and then it is used in the PAM demapping of br. The CD estimates the transmitted signal $x_j^{\bar{br}}$ based on the following MAP criteria

$$x_j^{\bar{br}} = \arg\max \Pr\left(x_j^{\bar{br}} \mid x'^{\bar{br}}_j\right) \tag{18}$$

which can also be written in the log-domain as

$$x_j^{\bar{br}} = \arg\min -\mathrm{LLh}\left(x_j^{\bar{br}}\right) - \sum_{c_{j,q(\bar{br})}=1} \lambda_{j,q(\bar{br})} \tag{19}$$

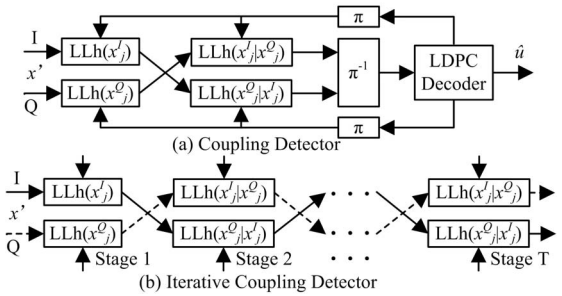

Fig. 4. Simplified detector implementation

where $c_{j,q(\bar{br})}$ are the bits mapping to $x_j^{\bar{br}}$. Compared with (8) for PAM, this MAP estimation has the similar complexity. The CD structure is depicted in Fig. 4(a). After the MAP estimation based on LLh $\left(x_j^{\bar{br}}\right)$, a one-dimensional PAM demapper based on LLh $\left(x_j^{br} \mid x_j^{\bar{br}}\right)$ is implemented to demap the br component. Similar manipulation is done for the demapping of $\bar{br}$ component. Compared with SD, one pre-stage is added in CD to estimate the CT for each component for better performance.

C. Iterative Coupling Detector

For the CD structure, if the first stage fails to give an accurate estimate of the noise n'^Q_j / n'^I_j, error is introduced in the second stage demapper and this will degrade the performance. This situation becomes worse when the noise correlation becomes stronger and the accuracy of the first stage estimation becomes lower since the CT is not considered in the estimation stage. Therefore, CD only works well in the weak-to-modest correlation situation. For stronger correlation, the iterative CD is proposed.

In CD, the estimation stage generates both LLh $\left(x_j^I \mid x_j^Q\right)$ and LLh $\left(x_j^Q \mid x_j^I\right)$. If LLh $\left(x_j^{\bar{br}}\right)$ in (19) is replaced by these LLh $\left(x_j^{\bar{br}} \mid x_j^{br}\right)$, the estimation of the transmitted signal $x_j^{\bar{br}}$ will be more accurate, since the CT information is involved. Therefore, if one more estimation stage is inserted between the first and the second stage of the CD, the detection performance can be improved due to the more accurate noise offset estimation from more accurate signal estimation. This insertion of additional signal estimation stage can be continued to further improve the detection performance as shown in Fig. 4(b). The extended CD is equivalent to two signal estimation loops respectively initialized by the estimation over LLh $\left(x_j^I\right)$ and LLh $\left(x_j^Q\right)$. Each of them iteratively estimates the signal x_j^I and x_j^Q based on LLh $\left(x_j^I \mid x_j^Q\right)$ and LLh $\left(x_j^Q \mid x_j^I\right)$. Instead of executing two estimation loops at the same time, only one of the two paths shown in Fig. 4(b) is executed in the proposed iterative CD. Either I or Q is selected to start the first-stage estimation based on the variance of $n'^I_j(n'^Q_j)$. The smaller the variance, the lower the probability that (19) gives an inaccurate estimation about x_j^I (x_j^Q). Therefore, we select the component that has the smaller noise variance as the initialization state. The iteration will stop when either there is no change on the noise estimate or the number of estimation stages exceeds a pre-defined threshold, T. Similar to CD, the last two estimation stages are also used to generate the demapping result.

TABLE I. COMPLEXITY COMPARISON OF THE DEMAPPERS

		EDC	ADD	COM
OD		$2M$	$0.5M\log_2 M + M$	M
SR	L	$1.5M$	$0.375M\log_2 M + 0.75M$	$0.75M$
	S	M	$0.25M\log_2 M + 0.5M$	$0.5M$
SD		$2\sqrt{M}$	$0.5\sqrt{M}\log_2 M + 2\sqrt{M}$	$2\sqrt{M}$
CD		$4\sqrt{M}$	$0.5\sqrt{M}\log_2 M + 4\sqrt{M}$	$4\sqrt{M}$
ICD	min	$3\sqrt{M}$	$0.5\sqrt{M}\log_2 M + 3\sqrt{M}$	$3\sqrt{M}$
	max	$T\sqrt{M}$	$0.5\sqrt{M}\log_2 M + T\sqrt{M}$	$T\sqrt{M}$

D. Complexity Comparison

For the MAP demapper used in an iterative receiver, the post processing operations in Fig. 3 and the noise property calculation in (13) are executed only once for each symbol. Hence, they are not the critical computations and are not considered in the complexity comparison. The critical computation includes the euclidean distance calculation (EDC) for the log-likelihood values in (6), (11), or (16), the additions (ADD) for combining the log-likelihood values with the apriori LLR in (8), and the comparisons (COM) for finding the minimum in (8). The required amount of these operations are measured for one symbol in one receiver iteration. Table I summarizes the comparison results under M-ary modulation for the SD, the CD, and the iterative CD (ICD). The complexity of the optimal demapper (OD) presented in section 2 and that of the sub-region (SR) method with the largest (L) and the smallest (S) region size [15] are also given for comparison. To simplify the comparison, the complexity of a 2-dimensional EDC is approximated by that of two 1-dimensional EDCs. The min and max for the ICD describes the lower and upper bound of its complexity as not all of the symbols consume all T stages. The minimum number of stages is equal to the initialization stage and 2 estimation stages. From the table, it is shown that the complexity of CD is much less than that of OD and SR for the higher order modulation, and the ICD complexity under a reasonable threshold value T is comparable to that of CD.

IV. SIMULATION RESULTS

Simulations are carried out on the DVB-T2 receiver using 256QAM and 64QAM as the modulation constellation. The bit interleaver and the SSD mapper are designed based on [11], in which constellation rotation angle $\alpha = \arctan(1/16)$ for 256QAM and $\alpha = 8.6$ degrees for 64QAM. Rate 1/2 LDPC code [11] with $N = 64800$ is adopted. The maximum iteration number is set to 49, and the maximum stages of ICD, T is set to 7. The FER performances are simulated for different demappers. Demappers based on sub-region (SR) simplification are also simulated. The original SR scheme proposed in [15] is not directly applicable for iterative receiver. Here we modified the SR so that it can be used in the iterative receiver. At the beginning of each demapping iteration, a hard decision is made based on the aposteriori probability of each symbol obtained from the previous decoding iteration to decide which sub-region to use.

Fig. 5 shows the frame error rate (FER) curves of OD, modified SR with the largest (SR-L) and the smallest (SR-S) region size, SD, CD, and ICD for 256 QAM. The performance

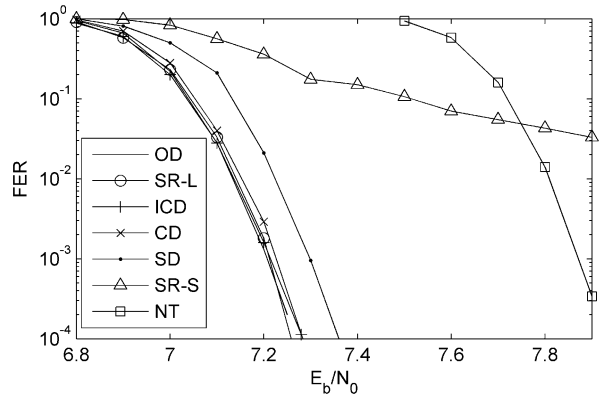

Fig. 5. FER of 256QAM

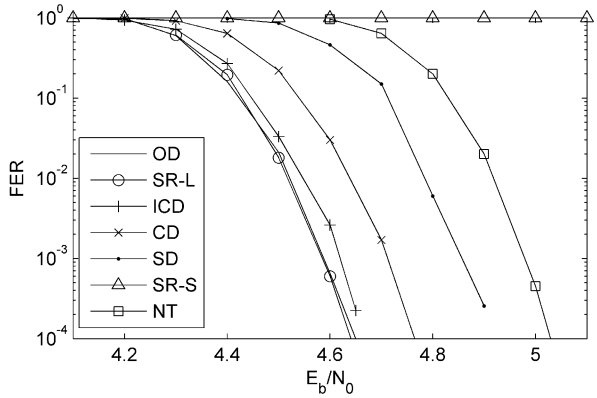

Fig. 6. FER of 64QAM

of the non-iterative (NT) receiver is also given as a reference. It shows that the SNR loss of SD is around 0.1 dB and that of CD is negligible. There is almost no SNR loss for ICD and SR-L. It is worthwhile to note that due to the limited sub-region size, SR-S even fails to converge in the iterative receiver. Since the noise correlation for 256QAM is small due to the smaller α, CD is almost sufficient to approach the performance of OD with a much less complexity.

Fig. 6 shows the FER curves for 64QAM. The performance of SR-L is even worse than that for 256QAM. Due to a larger α, the noise correlation is higher. Therefore, SD has a larger (around 0.3 dB) loss in SNR compared with 256QAM. Similarly, CD also loses more than 0.1 dB. In contrary, the degradation of the ICD with $T = 7$ is less than 0.02 dB.

Table II summarizes the complexity of different demappers for both 256 and 64QAM. The complexity is normalized with that of the OD of which the actual complexity numbers are also given. We can see that SR-L only reduces the complexity by 25%. While SR-S reduces the complexity by 50%, its FER performance is worse. For the SD and CD, the complexity is reduced by almost an order. For ICD, the complexity depends on the value of T. The complexity is relatively high for large T. However, not all the symbols in the ICD require all stages. We count the average number of stages required by the ICD for 64QAM and 256QAM. The average number for 64QAM ranges from 3.033 to 3.022 when E_b/N_0 ranges from 4.4 dB to 4.65 dB, and it ranges from 3.015 to 3.012 when E_b/N_0 ranges from 7 dB to 7.3 dB under 256QAM. It indicates that the average ICD stages is just slightly greater than the lower bound value shown in Table II. It means that most of the time, the symbols only need to use 3 stages for the demapping. Only in very rare case that it needs T stages. So the overall average complexity of ICD is even lower than that of CD.

TABLE II. COMPLEXITY COMPARISON FOR 256/64QAM

		256-QAM			64-QAM		
		EDC	ADD	COM	EDC	ADD	COM
	OD complexity	512	1280	256	128	256	64
normalized complexity	SR-L	0.75	0.75	0.75	0.75	0.75	0.75
	SR-S	0.5	0.5	0.5	0.5	0.5	0.5
	SD	0.0625	0.075	0.125	0.125	0.15625	0.25
	CD	0.125	0.1	0.25	0.25	0.21875	0.5
	ICD ($T = 3$)	0.09375	0.0875	0.1875	0.1875	0.1875	0.375
	ICD ($T = 7$)	0.21875	0.1375	0.4375	0.4375	0.3125	0.875

V. CONCLUSION

In this work, we propose several low-complexity rotated QAM demappers for DVB-T2 receiver. They are suitable to be used in iterative receiver structure. The complexity is reduced by more than 50% when comparing with the optimal demapper while the performance degradation is negligible.

REFERENCES

[1] G. Caire, et al., "Bit-interleaved coded modulation," *IEEE Trans. Inform. Theory*, vol. 44, no. 3, pp. 927-946, May 1998.

[2] J. Boutros and E. Viterbo, "Signal space diversity: a power and bandwidth-efficient diversity technique for the Rayleigh fading channel," *IEEE Trans. Inform. Theory*, vol. 44, no. 4, pp. 1453-1467, July 1998.

[3] A. Chindapol and J. A. Ritcey, "Design, analysis, and performance evaluation for BICM-ID with square QAM constellations in Rayleigh fading channels," *IEEE JSAC*, vol. 19, no. 5, pp. 944-957, May 2001.

[4] DVB-T2, "*Implementation guidelines for a second generation digital terrestrial television broadcasting system (DVB-T2)*", draft ETSI TR 102 831 V0.10.4, June 2010.

[5] R. G. Gallager, *Low-Density Parity-Check Codes*. Cambridge, MA: MIT Press, 1963.

[6] M. M. Mansour and N. R. Shanbhag, "High-throughput LDPC Decoders," *IEEE Trans. VLSI*, vol. 11, no. 6, pp. 976-996, Dec. 2003.

[7] S. ten Brink, "Designing iterative decoding schemes with the extrinsic information transfer chart," *AEO Int. J. Electron. Commun.*, vol. 54, no. 6, pp. 389-398, 2000.

[8] X. Li and J. A. Ritcey, "Bit-interleaved coded modulation with iterative decoding," *IEEE Commun. Letters*, vol. 1, no. 6, pp. 169-171, Nov. 1997.

[9] ____, "Bit-interleaved coded modulation with iterative decoding using soft feedback," *Electron. Letters*, vol. 34, no. 10, pp. 942-943, May 1998.

[10] Y. Li, et al., "Bit reliability mapping in LDPC-coded modulation systems," *IEEE Commun. Letters*, vol. 9, no. 1, pp. 1-3, Jan. 2005.

[11] DVB-T2, "*Frame structure channel coding and modulation for a second generation digital terrestrial television broadcasting system (DVB-T2)*", draft ETSI EN 302 755 V1.2.1, Feb. 2011.

[12] Y. Nana, et al., "Improved decoding of LDPC coded modulations," *IEEE Commun. Letters*, vol. 10, no. 5, pp. 375-377, May 2006.

[13] C. A. Nour and C. Douillard, "Improving BICM performance of QAM constellations for broadcasting applications," in *Proc. 5th Int. Symp. Turbo Codes and Related Topics*, pp. 55-60, 2008.

[14] M. Li, C. A. Nour, C. Jego, and C. Douillard, "Design of rotated QAM mapper/demapper for the DVB-T2 standard," *SiPS 2009: IEEE workshop on Signal Processing Systems*, pp. 18-23, Oct. 2009.

[15] D. Perez-Calderon, et al., "Rotated constellation demapper for DVB-T2," *Electron. Letters*, vol. 47, no. 1, pp. 31-32, Jan. 2011.

[16] M. Li, et al., "Efficient iterative receiver for bit-interleaved coded modulation according to the DVB-T2 standard," *ICASSP*, pp. 3168-3171, 2011.

[17] Y. Li, et al., "Simple iterative methods to exploit the signal-space diversity," *IEEE Trans. Commun.*, vol. 53, no. 1, pp. 32-38, Jan. 2005.

[18] N. H. Tran, et al., "Performance of BICM-ID with signal space diversity," *IEEE Trans. Wireless Commun.*, vol. 6, no. 5, pp. 1732-1742, May 2007.